A Convenient Organic–Inorganic Hybrid Approach Toward Highly Stable Squaraine Dyes with Reduced H-Aggregation

Zhengquan Yan, Hongyao Xu, Shanyi Guang, Xian Zhao, Weiliu Fan, and Xiang Yang Liu**

A generic and effective approach for solving the aggregation effect observed with optical materials in solid state or in a solution with a poor solvent was explored by designing two types of squaraine-containing polyhedral oligomeric silsesquoixane (POSS)-based hybrids. It is expected that incorporation of "huge" inorganic POSS nanoparticles into optical materials via covalent bonding can effectively decrease the strong dipole–dipole and π–π stacking interactions, inhibit intermolecular charge transfer between adjacent squaraine molecules, and improve optical, thermal and chemical stability of the resultant materials. Both theoretical calculations and experimental results indicate that the molecular design strategy is rational and efficacious. The resultant organic–inorganic hybrid optical materials effectively eliminate the aggregation of organic optical chromophoric groups by hindering intermolecular charge transfer and decreasing dipole–dipole and π–π stacking interaction between the chromophores, and exhibit good optical stability, i.e., the absorption peaks of H1 and H2 display only a slight blue-shift, even in the solid. Simultaneously, the hybrids also show significantly enhanced thermal, and chemical stabilities in comparison with the precursor organic optical materials.

1. Introduction

Optically absorbing materials have attracted extensive attention owing to their great potential applications in the fields of nonlinear optics, photodynamic therapy, optical data storage, laser printing, biological probes, infrared photography, solar cells, etc.[1,2] Among all the absorbing materials identified, i.e., phthalocyanines, metal complexes, polymethines, squaraines, radical dyes, and azo dyes,[3] squaraine dyes (SQ) are a particularly promising class of dyes widely applied in chemosensors,[4] bioimaging,[5] light-emitting diodes,[6] solar cells[7] etc. because of their intense absorption properties ($\varepsilon \geq 10^5$ L·mol^{-1}·cm^{-1}) from the red to the near-IR region. Nevertheless, the unique rigid zwitterionic structures of squaraines and the strong dipole–dipole and π–π stacking interactions between molecules often lead to the association/aggregation of SQ molecules in the solid state or in solutions that contain poor solvents for SQs, which further results in a strong optical-quenching effect associated with a red- or a blue-shift. These issues have greatly limited their practical applications in the optical field as absorbing materials.

To overcome molecular aggregation, it is found that increasing the chromophoric intermolecular distance may be an effective method; as described by Law, aggregation often occurs strongly when the distance between chromophoric molecules is ca. 3.5 Å due to an intermolecular charge transfer.[3] Thus, supramolecular encapsulating[8] and squaraine-derived-rotaxane strategies[5,9] were developed. Nevertheless, the above squaraine derivatives often suffer from inherent reversibility to squaraines themselves.[8] Additionally, the poor thermal and photostabilities of such derivatives turn out to be unfavorable factors for their application in the optical field.[4,5] Therefore, overcoming the effect of aggregation of chromophores and improving their thermal and optical stabilities at the same time remains a big challenge.

It is well-known that incorporation of nanosized inorganic particles, e.g., polyhedral oligomeric silsesquoixane (POSS, $R_xR_{8x'}$ Si_8O_{12}) with a well-defined nanosized cube-octameric structure,[10] into organic materials turns out to be an effective method for improving the thermal and photostability of the resultant materials.[11–15] We were inspired by Smith and co-workers' finding that aggregation of organic optical chromophores can be inhibited effectively when the interplanar distance of optical molecules is larger than ca. 7.0 Å.[9] Herein, we will explore a generic and effective approach to solve the issue of the aggregation of optical materials in the solid state or in solutions that contain poor solvents for the materials concerned, and also to improve their thermal and optical

Dr. Z. Yan, Prof. H. Xu, Prof. S. Guang, Prof. X. Y. Liu
College of Material Science and Engineering & State Key Laboratory for Modification of Chemical Fibers and Polymer Materials
Donghua University
Shanghai 201620, P. R. China
E-mail: hongyaoxu@163.com; phyliuxy@nus.edu.sg
Prof. X. Zhao, Prof. W. Fan
School of Chemistry and Chemical Engineering
Shandong University
Jinan, 250100, China
Prof. X. Y. Liu
Department of Chemistry and Department of Physics
Faculty of Science, National University of Singapore
2 Science Drive 3, 117542 Singapore

DOI: 10.1002/adfm.201101565

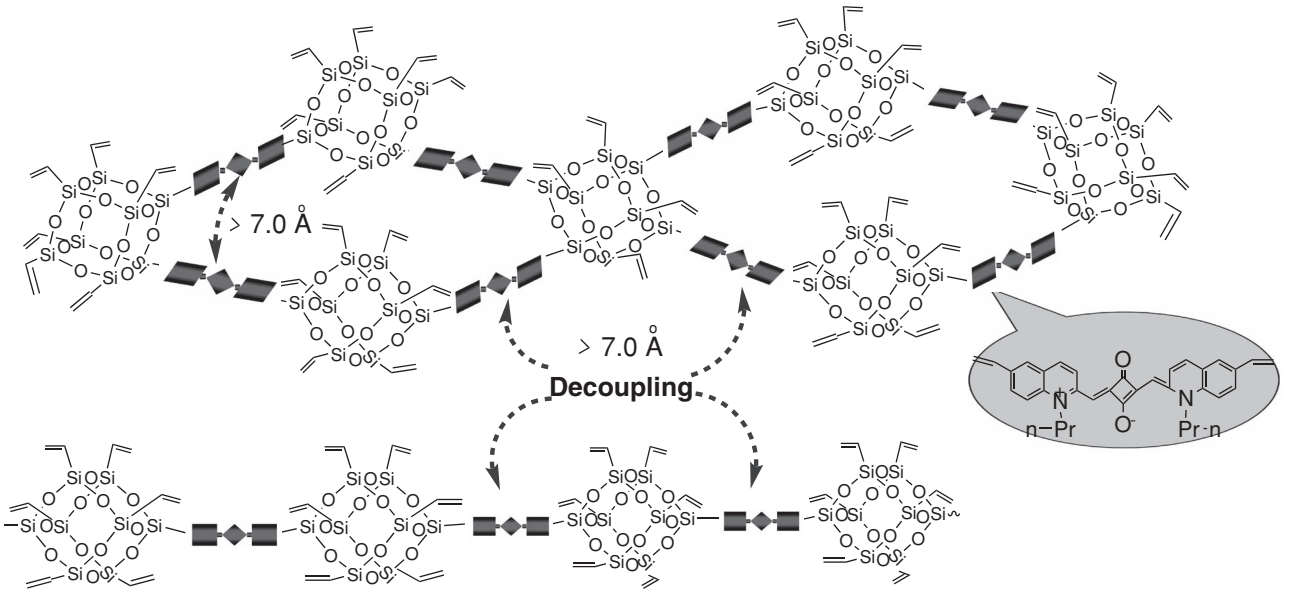

Scheme 1. Schematic illustration of nanosized spacer particles (POSS) introduced into squaraine (SQ) at molecular levels to suppress chromophoric aggregation.

stability by designing two kinds of SQ-containing POSS-based hybrids (H1 and H2) with different molecular architectures (see **Scheme 1**). The key strategy is to incorporate nanosized octavinyl-silsesquioxanes (OV-POSS) units into organic optical molecules through covalent bonding. It is expected that incorporation of "huge" inorganic POSS nanoparticles into SQ can effectively overcome the aggregation effect of SQ chromophoric groups by decreasing the strong dipole–dipole and π–π stacking interaction and inhibiting the intermolecular charge transfer between adjacent SQ molecules.

2. Results and Discussion

2.1. Theoretical Calculations

To validate the rationality of structural design of hybrid molecules, a theoretical calculation was conducted using the Gaussian 03 software suite with a B3LYP/6-31G level of theory,[16] which is used to understand the geometrical characters of the candidates. To simplify the calculation, the basic structural units of these two hybrids (H1 and H2) were selected and the bonds at the end of the structural units were saturated with hydrogen atoms. The calculated results are shown in **Figure 1**. It is striking that the average distances between chromophores in the basic structural units of H1 and H2 are found to be ca. 8.73 and 28.56 Å, respectively, which both fulfil the spacing requirement (>7.0 Å) for overcoming aggregation effectively,[9] i.e., incorporation of "huge" inorganic POSS nanoparticles into SQ via covalent bonding should be able to effectively suppress the aggregation effect owing to the increased interplanar distance between optical chromophoric groups (more than ca. 7.0 Å),[9] which may greatly decrease the dipole–dipole and π–π stacking interactions between the optical chromophores, and hinder intermolecular charge transfers.[3]

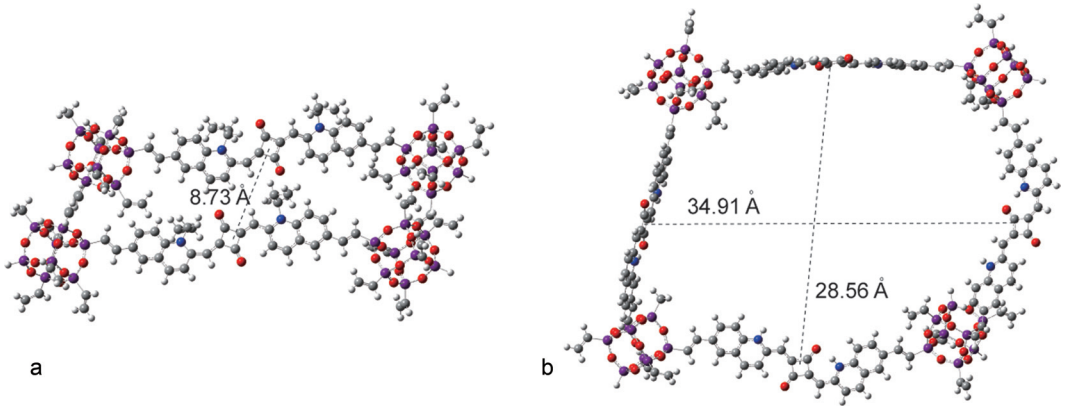

Figure 1. The optimized geometries of a) H1 and b) H2. Si, O, N, C, and H atoms are represented as purple, red, blue, gray, and white-gray, respectively.

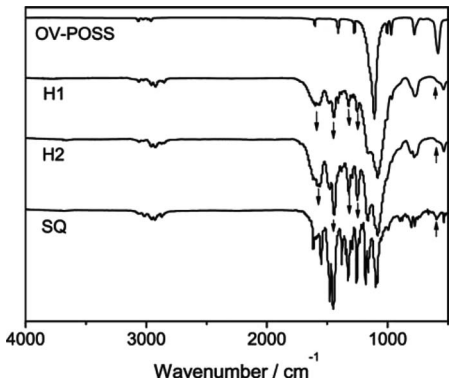

Figure 2. IR spectra of H1, H2, OV-POSS, and SQ.

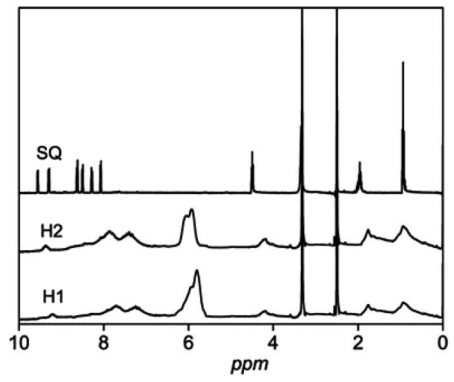

Figure 3. ^{1}H NMR spectra of SQ, H1, and H2.

2.2. Synthesis and Characterization

To experimentally verify the molecular design, H1 and H2 were prepared by a route based on the Heck reaction between OV-POSS and SQ with a molar feed ratio of 1:1 and 1:2, respectively.[17,18] H1 and H2 are soluble in some common organic solvents such as N,N-dimethylformamide (DMF), dimethylsulfoxide (DMSO), etc. However, the resultant hybrids are insoluble in these organic solvents when the molar feed ratio is greater than 1:2, i.e., 1:3 or 1:4.

To further confirm the structure of our products, we tried to use gas chromatography–mass spectrometry (GC-MS) methods to separate and verify the structure of the products, such as bead-type H1. GC-MS results indicated that a small amount of the variously substituted POSS forms (ca. 3 ~ 5 wt%) existed in the resulting product besides the main bead-type H1 (more than 90 wt%). Simultaneously, it was found that a little cross-linked by-product (less than 3 wt%) in our product was retained by the chromatogram column and badly contaminated the chromatographic system, which also suggests that it is difficult to separate and evaluate our products by chromatographic methods.

Therefore, herein we evaluate the resultant hybrid using gel permeation chromatography (GPC) methods. However, to protect the GPC system, the sample solutions in DMF (ca. 2 mg mL^{-1}) were filtered through 0.45-μm poly(tetrafluoroethylene) syringe-type filters before injection into the GPC system. Thereafter, the structure of the hybrids was deduced by means of GPC and spectral methods as follows.

The IR spectrum of SQ (**Figure 2**) shows characteristic bands at 1616, 1581, and 1449 cm^{-1} that are attributed to the aryl-ring stretching vibration, at 1317 and 1248 cm^{-1} to the C–O–C stretching vibration, and at 596 cm^{-1} to the C–Br stretching vibration. The IR spectrum of OV-POSS contains an intense characteristic Si–O stretching vibration at 1075 cm^{-1}. In the spectra of H1 and H2, the characteristic signals at 1616, 1581, 1449, 1317, and 1248 cm^{-1} corresponding to the SQ moiety emerge, and the C–Br stretching vibration at 596 cm^{-1} completely disappears after Heck reaction, which hints that Heck reaction was successful. Moreover, by taking the intensity of the Si–O stretching vibration peak at 1075 cm^{-1} as a standard, the intensity of all the characteristic bands corresponding to the SQ moiety at 1616, 1581, 1449, 1317, and 1248 cm^{-1} increases from H1 to H2 in proportion to the molar feeding ratio, which indicates that the number of substituent arms on POSS molecules increases with the molar feed ratio.

In the ^{1}H NMR spectra of H1 and H2 (**Figure 3**), we can see easily that all the characteristic signals at $\delta \approx$ 7.5–9.3, 4.2, 1.9, and 0.9 ppm corresponding to the SQ moiety and at $\delta \approx$ 5.9 ppm to the OV-POSS moiety emerge. However, the characteristic signals at $\delta \approx$ 7.5–9.3, 4.2, 1.9, and 0.9 ppm attributed to SQ moiety in H1 and H2 show a slight shift to high frequency because of the electron-donating effect of the POSS groups, which further confirms that the Heck reaction was successful. On the other hand, the characteristic singlet at $\delta \approx$ 5.9 ppm corresponding to the characteristic olefin proton of OV-POSS monomers turns into a doublet in the spectra of H1 and H2, with an integral area ratio of peak of ca. 2:6 for H1 and ca. 4:4 for H2, respectively, which further confirms that the molecular structures of the hybrids can be controlled by changing the molar feed ratio.[17,18] **Figure 4** shows the ^{29}Si NMR spectra of H1, H2, and OV-POSS. The spectrum of OV-POSS possesses a sharp characteristic singlet at ca. 79.3 ppm, while H1 displays two broad characteristic signals at ca. 70.0 and 80.0 ppm with an integral area ratio of ca. 2:6; this further confirms that the POSS molecules have reacted with squaraine molecules to yield a resultant

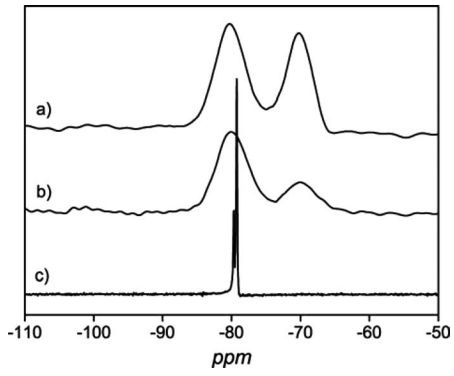

Figure 4. ^{29}Si NMR spectra of OV-POSS, H1, and H2.

hybrid with a bead-type structure. Similar to that of H1, the spectrum of H2 also displays two broad characteristic peaks at ca. 70.2 and 80.3 ppm with an integral area ratio of ca. 4:4, which supports the hypothesis that low-cross-linked network-type hybrids were obtained. This result is consistent with that from FTIR and ^{1}H NMR spectra, and a similar phenomenon is observed in our previous work.[17,18]

2.3. Decoupling Effect of the Hybrids

A red-shift or blue-shift in UV-vis spectra is commonly used to examine the aggregation effect in mixed DMSO–water solvents,[19] where DMSO is a good solvent and water is a poor solvent for SQ and the resultant optical hybrids. In this regard, the absorption spectra of H1, H2, and SQ in DMSO and in mixed DMSO–water solvents with different volume ratios were recorded. As shown in **Figure 5**a, both H1 and H2 have similar strong and sharp absorbance spectral profiles to that of the precursor SQ in DMSO solution. This observation means that all the molecules of H1, H2, and SQ are well-dispersed in their good solvents, so the intermolecular interaction is weak and no aggregation happens. The result also suggests that incorporation of "huge" inorganic POSS nano particles into organic optical materials has little influence on the inherent optical properties except that the maximal absorption peak red-shifts by 21 nm for H1 and 27 nm for H2, compared to that of SQ (λ_{max} = 739 nm), respectively. These red-shifts originate from the σ–π conjugation between the Si atom of POSS and the chromophore in the hybrids.[20]

In a 1:1 (v/v) DMSO–water mixed solvent, the absorption spectrum of SQ is obviously broad and displays a prominent blue-shift from 739 nm (the λ_{max} of SQ in pure DMSO) to 590 nm. When a 1:9 (v/v) DMSO–water mixed solvent is used, the absorption peak of SQ shows a further blue-shift to 560 nm with great spectral quenching. This result means that the optical properties of SQ are not stable in poor solvents, even in a mixed solvent containing a small fraction of the poor solvent, i.e., SQ easily forms H-type aggregates resulting from intermolecular charge transfers, strong dipole–dipole, and π–π stacking interactions.[3] However, it is surprising that the absorption peaks of H1 and H2 in a 1:1 (v/v) DMSO–water mixed solvent exhibit almost no notable change (Figure 5b and Figure 5c). Even in a 1:9 (v/v) DMSO–water mixed solvent, the absorption peaks of both H1 and H2 only show a minor blue-shift by only 9 and 7 nm, respectively, which hints that the H-aggregation of the SQ moiety in H1 and H2 is largely eliminated, i.e., both H1 and H2 are optically stable, and that incorporation of large inorganic POSS nanoparticles into SQ can effectively hinder charge transfer and attenuate strong dipole–dipole and π–π stacking interactions between SQ molecules, and so eliminate their aggregation. The method of using huge nanoparticles as a structural unit to construct a molecular architecture for overcoming the aggregation effect has never been reported before as far as we know.

It is well known that SQ in the solid state forms H-aggregates much more easily than that in a dilute solution, which leads to a blue-shift of the absorbance spectrum; it also forms J-aggregates more easily, which results in a red-shift of the absorbance spectrum with a broader half-peak width than that in a dilute

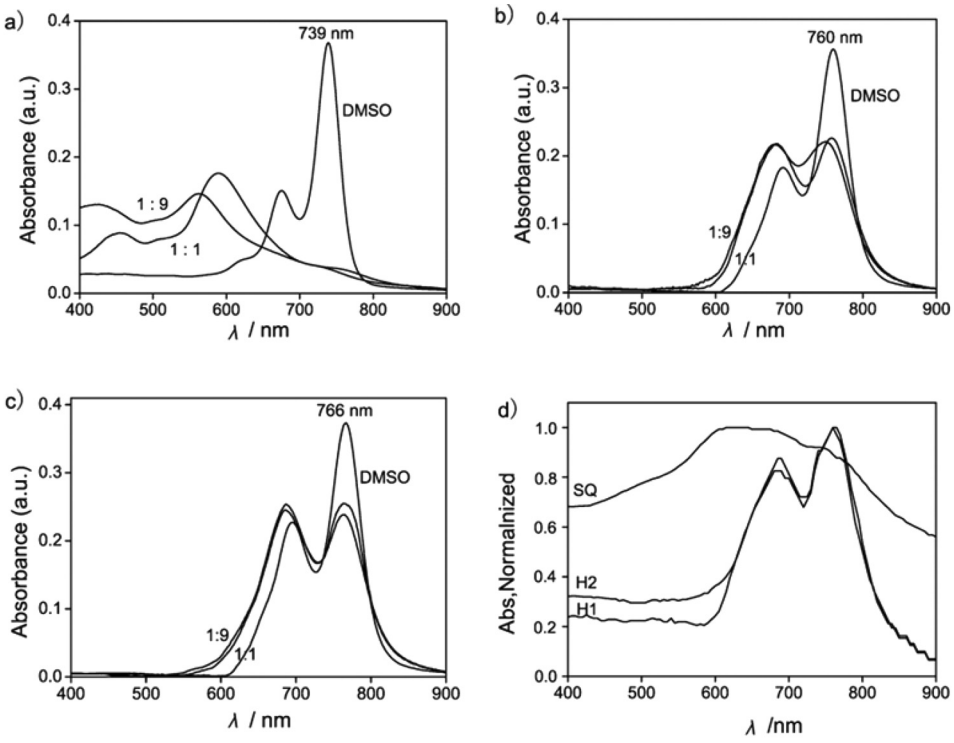

Figure 5. Partial absorption spectra of a) SQ, b) H1, and c) H2 in DMSO, DMSO–water (1:1, v/v), and DMSO–water (1:9, v/v) and d) absorption spectra of SQ, H1, and H2 in solid-state films from DMSO.

solution. To further verify the rationality of our molecular design, the UV-vis spectra of H1, H2, and SQ in their solid films were recorded and are shown in Figure 5d. From Figure 5d, it can be seen that, in the spectrum of solid SQ, an obvious blue-shift of absorption peak from 739 to 578 nm with a wider half-peak width of ca. 320 nm was observed than in solution, i.e., this optical property of SQ is extremely unstable and shows a much weaker and broader absorption band with a larger blue-shift in the solid film than that in dilute solution. This result may be attributed to the presence of H-type aggregates owing to the unique rigid zwitterionic structure which results in strong dipole–dipole and π–π stacking interactions and intermolecular charge transfer. Nevertheless, the absorption peaks of H1 and H2 only display a slight blue-shift of ca. 10 nm and the optical absorption intensity is almost unchanged, which further confirms that both H1 and H2 in the solid are still optically stable. This stability may be attributed to the larger distances between chromophores (ca. 8.73 Å for H1 and ca. 28.56 Å for H2, Figure 1), which effectively eliminate the dipole–dipole and π–π stacking interactions between adjacent optical chromophores, and so suppress intermolecular charge transfers. The results further support Smith and co-workers' conclusion that aggregation of organic optical chromophores can be inhibited effectively when the interplanar distance of optical molecules is larger than ca. 7.0 Å.[9] At the same time, the insulation of inorganic POSS is another important factor that may interrupt charge transfer between the conjugated chromophores significantly.[21]

2.4. Thermal Stability

The thermal stabilities of the hybrids (H1 and H2) and the precursors SQ and OV-POSS were estimated by using thermogravimetric analysis (TGA) under nitrogen at a heating rate of 10 °C·min^{-1}. The results are shown in **Figure 6**. The thermal decomposition temperatures (T_d, 5 wt% loss) of H1, H2, SQ, and OV-POSS were 352 °C, 315 °C, 194 °C and 240 °C, respectively. Namely, the T_d values of the hybrids H1 and H2 are strikingly elevated by 158 °C and 121 °C, respectively, in comparison with that of SQ, and demonstrate that incorporation of large inorganic POSS nanoparticles into organic optical materials effectively enhances the thermal stability of the resulting functional

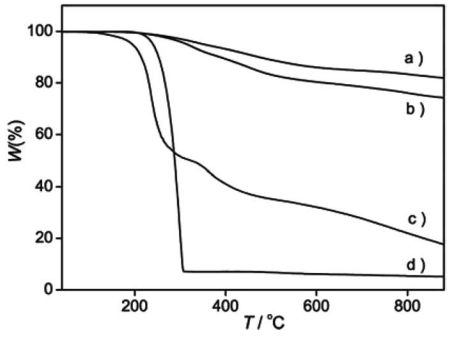

Figure 6. TGA thermograms of a) H1, b) H2, c) SQ, and d) OV-POSS at a ramp rate of 10 °C min^{-1} in nitrogen flow.

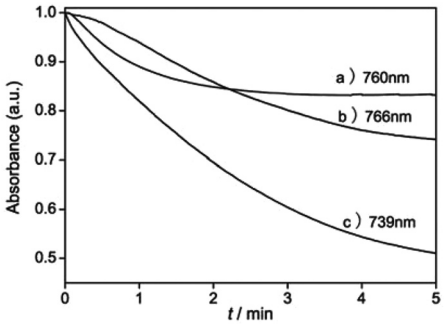

Figure 7. Change in absorption upon addition of cysteine (5 mM) to 5 μM solutions of a) H1, b) H2, and c) SQ in DMSO at 25 °C.

hybrids. This observation may be attributed to the barrier effect of inorganic POSS by limiting heat transfer, which protects the underlying material from heat attack. Simultaneously, the vibration hindrance of organic segments connected covalently to nanosized bulk POSS is also an important factor that results in thermal stabilization,[22,23] in spite of the decomposition of POSS in the surface of H1 and H2, which will yield highly thermally stable SiO_2 in the surface that will further protect the underlying materials from heat attack.[24] A similar result was found in previous publications.[11–15]

2.5. Chemical Stability

The chemical stability of the hybrids was also investigated. To achieve this goal, separate samples of H1, H2, and SQ in DMSO were treated with excess cysteine at room temperature. The subsequent time-dependence of the absorption changes is shown in **Figure 7**. After 5 min treatment with excess cysteine, the absorption intensity of SQ at 739 nm decreased from 1 to 0.49, while those of H1 at 760 nm and H2 at 766 nm only decreased from 1 to 0.85 and 0.74, respectively, which indicates that their chemical stability is in the order: H1 > H2 > SQ, and the chemical stability of the hybrids is significantly enhanced over that of the precursor, which may be attributed to the steric protection provided by the huge cagelike POSS[25] as well as the insulation of inorganic POSS[21] which hinders electron transport between organic chromophore molecules.

2.6. Photostability

The photostability of H1, H2, and SQ in DMSO was also examined. The samples were placed 100 cm away from a 1000 W iodine–tungsten lamp in a glass holder and with the temperature maintained at 25 °C by use of a cold trap. During irradiation, the absorption spectra of H1, H2, and SQ in DMSO were recorded every 4 hours; the results are given in **Figure 8**. Similar to their chemical stability, an enhancement effect in photostability is observed for H1 and H2 over SQ, which increases with POSS content owing to the barrier of oxidatively stable POSS[24] as well as the insulation of inorganic POSS[21] nanoparticles, for which photo-oxidation is unfavorable.

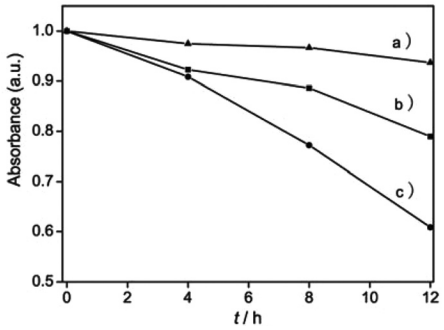

Figure 8. Curves of absorbance at λ_{max}–time under irradiation from a 1000 W iodine–tungsten lamp of a) H1, b) H2, and c) SQ in DMSO at 25 °C.

3. Conclusions

In conclusion, incorporation of "huge" inorganic POSS nanoparticles into organic optical materials via covalent bonding at the molecular level can effectively overcome the aggregation effect of organic chromophoric groups, and significantly enhance their thermal, chemical, and photo stability. We provide a generic and effective strategy to prepare optical stable materials with high thermal and photostability. Notice that only some of the eight vinyl functional groups in octafunctional POSS in the hybrids (H1 and H2) are occupied. The rest of the vinyl groups also provide opportunities for further incorporation of other functional groups, which may allow building-in of additional functions to the hybrids in the future.

4. Experimental Section

As shown in **Scheme 2**, the hybrids (H1, H2) were designed and synthesized through a multistep reaction route.

Synthesis of 6-Bromo-quinaldine: To a 100-mL three-necked bottle was added hydrochloric acid solution (44.8 mL, 6 mol L^{-1}), 4-bromoaniline (1535 mg, 8.9 mmol), and acetic acid (0.5 mL, 8.9 mmol). The formed mixture was refluxed at 100 °C for 0.5 h, followed by addition of iodine/potassium (50 mg/132 mg, 0.4 mmol/0.8 mmol) and toluene (10 mL). Then a mixture of toluene (2 mL) and crotonaldehyde (1.5 mL, 17.8 mmol) was added dropwise over a period of 1 h and the resulting mixture refluxed for another 6 h, before cooling to room temperature, and making alkaline using ammonia solution to induce complete precipitatation. The precipitate was filtered and purified by column chromatography on silica gel (eluent: petroleum ether/ethyl acetate = 1:6) to afford 1.76 g (89%) 6-bromo-quinaldine as a light yellow crystal; IR (KBr): ν = 3048 (C–H), 1596, 1488, 1463 (Ar), 637 cm^{-1} (C–Br); ^{1}H NMR (400 MHz, DMSO-d_6, δ): 7.97 (d, J = 8.4 Hz, 1 H, H^4), 7.90 (s, 1 H, H^5), 7.76 (d, J = 7.4 Hz, 1 H, H^8), 7.74 (d, J = 7.0 Hz, 1 H, H^3), 7.31 (d, J = 8.8 Hz, 1 H, H^5), 2.74 (s, 3 H, CH_3); Calcd. for $C_{10}H_8NBr$: C 50.08, H 3.63, N 6.03; Found: C 60.17, H 3.77, N 6.14.

Synthesis of N-Propyl-6-bromo-quinaldinium Salt: A mixture of 6-bromo-quinaldine (666 mg, 3 mmol), propyl iodide (1.7 g, 10 mmol), and 2 mL acetonitrile was heated in a sealed tube at 100 °C–105 °C for 12 h. The formed precipitate was filtered, washed thoroughly with cold diethyl ether, and purified by column chromatography on silica gel (eluent: petroleum methanol/chloroform = 1:4) to afford 0.72 g (61%) *N*-propyl-6-bromo-quinaldinium salt as a light green crystal; IR (KBr): ν = 3019, 2956, 2870 (C–H), 1601, 1509, 1466 (Ar), 598 cm^{-1} (C–Br); ^{1}H NMR (400 MHz, DMSO-d_6, δ): 8.68 (d, J = 8.2 Hz, 1 H, H^4), 8.53 (d, J = 8.5 Hz, 1 H, H^3), 8.35 (s, 1 H, H^5), 8.05 (d, J = 5.7 Hz, 1 H, H^8), 7.83 (d, J = 8.5 Hz, 1 H, H^5), 3.98 (t, J = 7.7 Hz, 2 H, $CH_2CH_2CH_3$), 2.84 (s, 3 H, CH_3), 1.91 (m, J = 7.5 Hz, 2 H, $CH_2CH_2CH_3$), 1.15 (t, J = 2.9 Hz, 3H, $CH_2CH_2CH_3$); Calcd. for $C_{13}H_{14}NBrI$: C 39.93, H 3.61, N 3.58; Found: C 40.03, H 3.67, N 3.54.

Synthesis of 6-Bromo-quinaldine Squaraine Dye (SQ): A mixture of *N*-propyl-6-bromo-quinaldinium salt (784 mg, 2 mmol), squaric acid (114 mg, 1 mmol), and quinoline (1 mL) was refluxed in a mixture of n-butanol and toluene in the ratio of 1:1 (v/v, 15 mL) with azeotropic removal of water for 24 h. The solvent was removed by distillation under reduced pressure to obtain a residue which was purified by column chromatography on silica gel (eluent: methanol/chloroform = 1:9) to afford 1.48 g (86%) of SQ as a dark green crystal; IR (KBr): ν = 3016, 2953, 2872 (C–H), 1616, 1581, 1449 (Ar), 1317, 1248 (O–C–O), 596 cm^{-1} (C–Br); ^{1}H NMR (400 MHz, DMSO-d_6, δ): 9.56 (d, J = 5.7 Hz, 2 H, H^4), 9.30 (d, J = 6.4 Hz, 2 H, H^9), 8.63 (d, J = 9.2 Hz, 2 H, H^3), 8.50 (d, J = 8.0 Hz, 2 H, H^8), 8.30 (s, 2 H, H^5), 8.07 (d, J = 7.8 Hz, 2 H, H^7), 4.49 (t, J = 7.5 Hz, 4 H, $CH_2CH_2CH_3$). 1.95 (m, J = 7.5 Hz, 4 H, $CH_2CH_2CH_3$), 0.95 (t, J = 2.6 Hz, 6 H, $CH_2CH_2CH_3$); Calcd. for $C_{30}H_{27}N_2Br_2O_2$: C 59.33, H 4.48, N 4.61; Found: C 59.24, H 4.57, N 4.69.

Synthesis of POSS-Based Hybrids: The POSS-based hybrids were prepared with different molar feed ratio of SQ (*x*) to OV-POSS (*y*), by a conventional Heck reaction using $Pb(Ac)_2$ as a catalyst, K_2CO_3 as an acid binding agent, and *N*,*N*-dimethyl glycine (DMG) as a ligand at ca. 130 °C in dry *N*-methyl pyrrolidone. For H1, *x*:*y* was 1:1 and *x*:*y* was 1:2 for H2. The reactions were carried out under a nitrogen atmosphere, using a vacuum-line system. Taking the synthesis of bead-type structural hybrid H1 as an example, a mixture of SQ (121 mg, 0.2 mmol), OV-POSS (127 mg, 0.2 mmol), DMG (123 mg, 1.2 mmol), palladium acetate (16 mg, 0.06 mmol), and K_2CO_3 (83 mg, 0.6 mmol) was placed in a 50-mL sealed three-necked bottle; the bottle was evacuated under vacuum and then flushed with dry nitrogen three times. After 5 mL of freshly distilled *N*-methyl pyrrolidone was added, the reaction mixture was refluxed at 130 °C under nitrogen for 10 h and then cooled to room temperature. The mixture was then diluted with 50 mL of water and filtered. The precipitate was washed with toluene first, and then redissolved in minimal DMSO. The DMSO solution was added dropwise into 100 mL of H_2O to precipitate the hybrids. This purification procedure was repeated three times.

The hybrid H2 was prepared by a similar method with a feed ratio of SQ and OV-POSS of 2:1.

H1: Dark brown powder; M_n = 1720, PDI, 1.20, (GPC, polystyrene); Yield: 57%; IR (KBr): ν = 3058, 2957, 2876 (C–H), 1600, 1572, 1447 (Ar), 1111 (Si–O–Si), 760 cm^{-1} (C–Si); ^{1}H NMR (400 MHz, DMSO-d_6, δ): 9.17 (br, H, H^4), 7.71 (br, H, H, $H^{3,5,9}$), 7.21 (br, H, $H^{7,8}$), 5.82 (br, H, POSS–C*H*=C*H* and C*H*=CH_2), 4.20 (br, H, $CH_2CH_2CH_3$), 1.77 (br, H, $CH_2CH_2CH_3$), 0.93 (br, H, $CH_2CH_2CH_3$); ^{29}Si NMR (79.49 MHz, solid, δ): –70.15 (s, Si–CH=CHR), –80.11 (s, Si–CH=CH_2).

H2: Dark brown powder; M_n = 2010, PDI, 1.24 (GPC, polystyrene); Yield: 51%; IR (KBr): ν = 3053, 2955, 2885 (C–H), 1600, 1565, 1483 (Ar), 1104 (Si–O–Si), 759 cm^{-1} (C–Si); ^{1}H NMR (400 MHz, DMSO-d_6, δ): 9.36 (br, H, ArH, H^4), 7.84 (br, H, $H^{3,5,9}$), 7.40 (br, H, $H^{7,8}$), 5.92 (br, H, POSS–C*H*=C*H* and C*H*=CH_2), 4.19 (br, H, $CH_2CH_2CH_3$), 1.76 (br, H, $CH_2CH_2CH_3$), 0.93 (br, H, $CH_2CH_2CH_3$); ^{29}Si NMR (79.49 MHz, solid, δ): –70.25 (s, Si–CH=CHR), –80.27 (s, Si–CH=CH_2).

Supporting Information

Supporting Information is available from the Wiley Online Library or from the author.

Acknowledgements

The authors gratefully acknowledge financial support from the National Natural Science Fund of China (Grant Nos. 20974018, 20971021, 51073031, and 21171034), National Oversea Scholar Cooperation

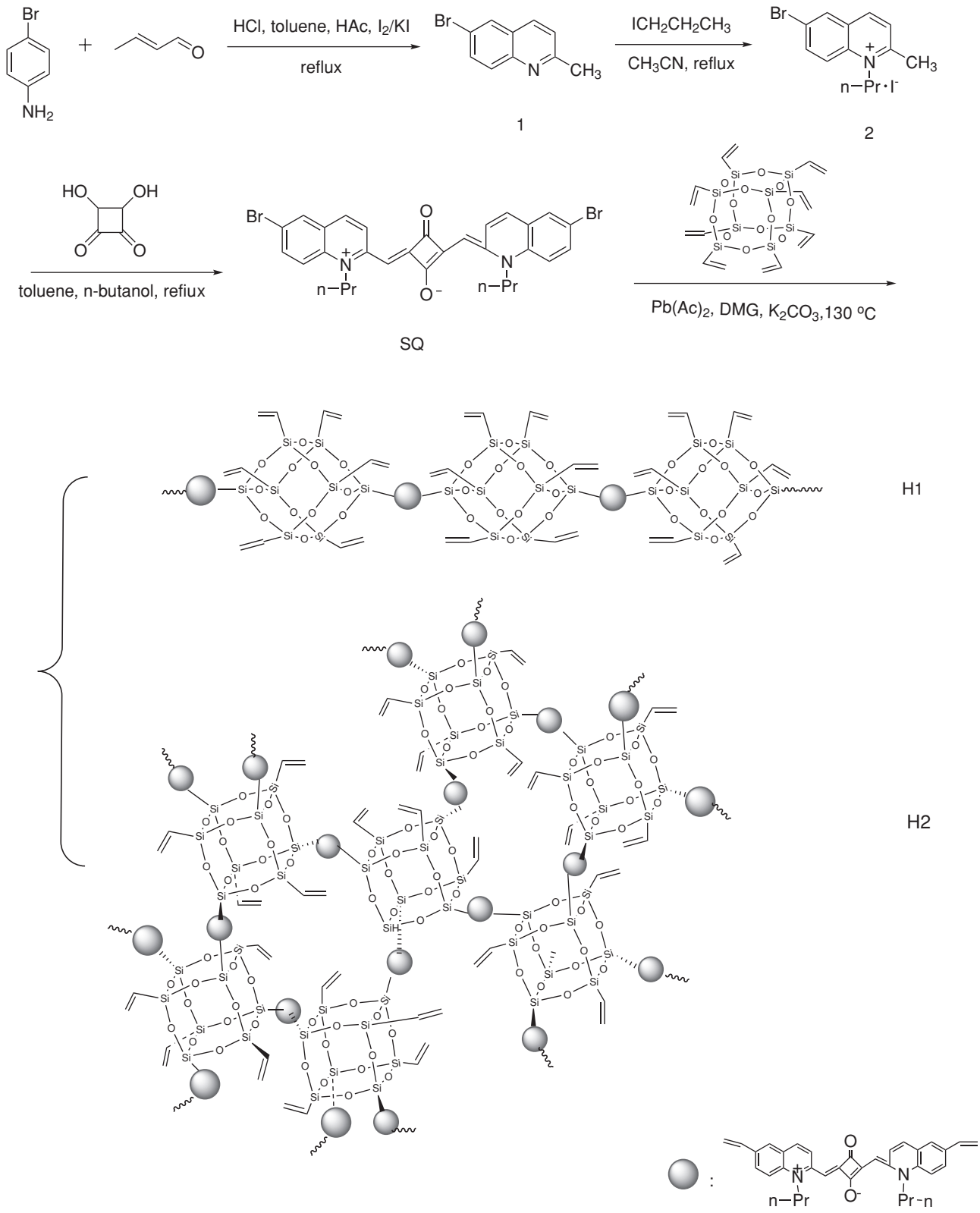

Scheme 2. The synthetic routes of the hybrids (H1 and H2).

Research Fund of China (No. 50928301), Ph.D. Program Foundation of Ministry of Education of China (No.20070255012), Shanghai Leading Academic Discipline Project (No. B603), and the Program of Introducing Talents of Discipline to Universities (No.111-2-04).

Received: July 11, 2011
Published online: November 17, 2011

[1] H. J. Snaith, *Adv. Funct. Mater.* **2010**, *20*, 13.
[2] T. Geiger, S. Kuster, J.-H. Yum, S.-J. Moon, M. K. Nazeeruddin, M. Grätzel, F. Nüesch, *Adv. Funct. Mater.* **2009**, *19*, 2720.
[3] K.-Y. Law, *Chem. Rev.* **1993**, *93*, 449.
[4] Z. Q. Yan, S. Y. Guang, H. Y. Xu, X. Y. Liu, *Analyst* **2011**, *136*, 1916.
[5] J. J. Gassensmith, J. M. Baumes, B. D. Smith, *Chem. Commun.* **2009**, 6329.
[6] J. Q. Qu, J. Y. Zhang, A. C. Grimsdale, K. Mullen, F. Jaiser, X. H. Yang, D. Neher, *Macromolecules* **2004**, *37*, 8297.
[7] Z. S. Wang, N. Koumura, Y. Cui, M. Takahashi, H. Sekiguchi, A. Mori, T. Kubo, A. Furube, K. Hara, *Chem. Mater.* **2008**, *20*, 3993.
[8] S. T. Das, K. G. George, P. V. Kamat, *J. Chem. Soc. Faraday Trans.* **1992**, *88*, 3419.
[9] E. Arunkumar, C. C. Forbes, B. C. Noll, B. D. Smith, *J. Am. Chem. Soc.* **2005**, *127*, 3288.
[10] Y. Xu, S.-W. Kuo, J.-S. Lee, F.-C. Chang, *Macromolecules* **2002**, *35*, 8788.
[11] P. T. Mather, H. G. Jeon, A. Romo-Uribe, T. S. Haddad, J. D. Lichtenhan, *Macromolecules* **1999**, *32*, 1194.
[12] H. Y. Xu, B. H. Yang, J. F. Wang, S. Y. Guang, C. Li, *Macromolecules* **2005**, *38*, 10455.
[13] X. Wang, S. Y. Guang, H. Y. Xu, X. Y. Su, X. Zhu, C. Li, *J. Polym. Sci., Part A: Polym. Chem.* **2010**, *48*, 1406.
[14] H. Y. Xu, B. H. Yang, J. F. Wang, S. Y. Guang, C. Li, *J. Polym. Sci., Part A: Polym. Chem.* **2007**, *45*, 5308.
[15] X. Y. Su, C. W. Li, H. Y. Xu, X. Y. Liu, X. Wang, Y. L. Song, *Macromolecules* **2010**, *43*, 2840.
[16] M. J. Frisch, G. W. Trucks, H. B. Schlegel, G. E. Scuseria, M. A. Robb, J. R. Cheeseman, J. A. J. Montgomery, T. Vreven, K. N. Kudin, J. C.Burant, J. M. Millam, S. S. Iyengar, J. Tomasi, V. Barone, B. Mennucci, M. Cossi, G. Scalmani, N. Rega, G. A. Petersson, H. Nakatsuji, M. Hada, M. Ehara, K. Toyota, R. Fukuda, J. Hasegawa, M. Ishida, T. Nakajima, Y. Honda, O. Kitao, H. Nakai, M. Klene, X. Li, J. E. Knox, H. P. Hratchian, J. B. Cross, V. Bakken, C. Adamo, J. Jaramillo, R. Gomperts, R. E. Stratmann, O. Yazyev, A. J. Austin, R. Cammi, C. Pomelli, J. W. Ochterski, P. Y. Ayala, K. Morokuma, G. A. Voth, P. Salvador, J. J. Dannenberg, V. G. Zakrzewski, S. Dapprich, A. D. Daniels, M. C. Strain, O. Farkas, D. K. Malick, A. D. Rabuck, K. Raghavachari, J. B. Foresman, J. V. Ortiz, Q. Cui, A. G. Baboul, S. Clifford, J. Cioslowski, B. B. Stefanov, G. Liu, A. Liashenko, P. Piskorz, I. Komaromi, R. L. Martin, D. J. Fox, T. Keith, M. A. Al-Laham, C. Y. Peng, A. Nanayakkara, M. Challacombe, P. M. W. Gill, B. Johnson, W. Chen, M. W. Wong, C. Gonzalez, J. A. Pople, *Gaussian 03, revision A.1*; Gaussian, Inc., Pittsburgh, PA, **2004**.
[17] X. Y. Su, S. Y. Guang, H. Y. Xu, X. Y. Liu, S. Li, X. Wang, Y. Deng, P. Wang, *Macromolecules* **2009**, *42*, 8969.
[18] B. H. Yang, H. Y. Xu, Z. Z. Yang, X. Y. Liu, *J. Mater. Chem.* **2009**, *19*(47), 9038.
[19] H. J. Chen, M. S. Farahat, K. Y. Law, D. G. Whitten, *J. Am. Chem. Soc.* **1996**, *118*, 2584.
[20] K. Y. Pu, K. Li, B. Liu, *Adv. Mater.* **2010**, *22*, 643.
[21] J. M. Kang, H. J. Cho, J. Lee, J. I. Lee, S. K. Lee, N. S. Cho, D. H. Hwang, H. K. Shim, *Macromolecules* **2006**, *39*, 4999.
[22] M. Z. Asuncion, R. M. Laine, *Macromolecules* **2007**, *40*, 555.
[23] E. Markovic, J. Matisons, M. Hussain, G. P. Simon, *Macromolecules* **2007**, *40*, 2694.
[24] A. S. Brown, *Aerospace America* **1999**, *37*, 30.
[25] C. H. Chou, S. L. Hsu, K. Dinakaran, M. Y. Chiu, K. H. Wei, *Macromolecules* **2005**, *38*, 745.